Solar radiation and ice melting in Lake Vendyurskoe, Russian Karelia

M. Leppäranta, A. Terzhevik and K. Shirasawa

ABSTRACT

Field experiments were conducted during two melting periods, April 2006 and April 2007, in Lake Vendyurskoe. The observation programme included weather, ice and snow thickness and structure, water temperature and solar radiation transfer through the ice. Albedo showed a systematic decrease from 0.5–0.8 for wintertime dry ice and snow to 0.1 for wet bare ice in spring, with spatial standard deviation of about 10%. The e-folding depth of light level was 60–80 cm for congelation ice and 15 cm for snow-ice. Light transmissivity of the ice cover increased from melting but decreased from ice deterioration; it varied between 0.25–0.35 in 2006, while in 2007 there was a systematic trend from 0.1 to 0.5 in six days. The heat budget was governed by net solar radiation with daily peaks up to 400–500 W m^{-2} on clear days. The average daily melt was 1.2 cm at the surface, 0.5 cm at the bottom and 1–2 cm (thickness equivalent) in the interior.

Key words | albedo, lake ice, melting, solar radiation, transmissivity

M. Leppäranta (corresponding author)
Department of Physics,
University of Helsinki,
P.O. Box 48,
Helsinki FI-00014,
Finland
E-mail: *matti.lepparanta@helsinki.fi*

A. Terzhevik
Northern Water Problems Institute,
Karelian Research Centre, Russian Academy of Sciences,
Petrozavodsk,
Russia

K. Shirasawa
Institute of Low Temperature Science,
Hokkaido University,
Sapporo,
Japan

INTRODUCTION

Boreal lakes have a seasonal ice cover. Ice grows to the order of 0.5 m thickness in winter and melts for about one month in March–June, depending on the location. In the melting period the heat budget is governed by the radiation balance, with occasional events with large turbulent fluxes or liquid precipitation in between. Due to weakening of the ice, technical problems and safety issues bring difficulties for fieldwork, and consequently not many *in situ* investigations have been made. However, to understand the annual cycle of freezing lakes such work is critically needed.

Solar radiation has a major role in the melting of lake ice. It is the leading heat flux, and is the only source term for the internal melting and deterioration of the ice (e.g. Leppäranta 2009). A significant amount of solar radiation also penetrates the ice sheet and warms the water beneath the ice, initiating convection and primary production and also contributing to the melting of the bottom. The strength of the spring overturn depends on the conditions in the melting period. To quantify the influence of the solar radiation, the key parameters are the albedo and the light attenuation coefficient. During the melting period, dictated by the evolving characteristics of the ice and snow, both of these parameters show large space–time variability, which is not yet well understood.

Ice cover acts as a filter for the solar radiation, lowering the radiation level and modifying the radiation spectrum. The albedo ranges from 0.9 for new snow, around 0.5 for bare ice and down to 0.06 for open water (e.g. Arst *et al.* 2006). Basically, just the visible light band penetrates into the ice, and the magnitude of the light attenuation depth (defined as the e-folding depth of downwelling planar irradiance) is 1 m in liquid lake water, 0.1–1 m in frozen lake water and 0.05–0.1 m in snow. The transparency of the ice and snow depends on the gas bubbles and the ice crystal structure. Clear, bubble-free ice can be even more transparent than the liquid water in the same lake, but the attenuation depth of snow-ice and snow is of the order of 0.1 m (e.g. Wang *et al.* 2005; Arst *et al.* 2006).

doi: 10.2166/nh.2010.122

To improve the understanding of the ice melting period, field campaigns were conducted in Lake Vendyurskoe, Russian Karelia, in April 2006 and April 2007. The programme included observations of snow and ice thickness and structure, solar radiation transfer through the ice and weather. The main purposes were to examine the evolution of the albedo and the light attenuation coefficient in the ice and snow, ice melt rates on the top surface, bottom surface and the interior and the light conditions beneath the ice cover in the melting period. The results of these investigations are presented here. The albedo generally decreased during the melting period due to the disappearance of snow and the formation of liquid water on and in the ice sheet, while light attenuation showed a maximum before water filled melt pores. The top, bottom and interior melt rates were of the same order of magnitude dictated by the optical properties of the ice and relative proportion of solar heating in the energy budget.

FIELD SITE AND DATA

Lake Vendyurskoe

Lake Vendyurskoe is located in the rectangle 62°10′–62°20′N × 33°10′–33°20′E in Russian Karelia. The lake hollow is of glacial origin. Vendyurskoe is a mesotrophic lake, the conductivity of the water is 18–20 μS cm^{-1}. The water is humic as is typical in Karelia but not strongly so, and the Secchi depth is 3–4 m. The lake is small and shallow, elongated from west to east with length 7 km, width 1.5 km, area 10.4 km^2 and the mean and maximal depths are 5.3 m and 13.4 m (Litinskaya & Polyakov 1975). The inflow is small and governed by precipitation and groundwater flux, and the Suna River takes the outflow into Lake Onega. Bottom sediments are composed of sand at shallow (2–3 m) depths and of brown and dark-brown silts in deeper parts. The silt thickness reaches 0.4–1.0 m (Litinskaya & Polyakov 1975). The organic matter content varies from 10% in sand to 30–50% in silty bottom sediments in the shallow northwest part of the lake.

The ice cover in Lake Vendyurskoe typically forms in the first half of November; the range is from late October to the beginning of December. The lake then becomes ice-free by 10–20th of May. The ice-covered period therefore lasts for 180–190 days (Petrov *et al.* 2005). The ice surface is covered with snow over most of the winter, with thickness gradually increasing to its maximum (20–25 cm) in mid-winter. With the onset of melting, the snow depth rapidly decreases and disappears by late April. In mid-April, the thicknesses of snow and ice are usually 0–9 cm and 60–69 cm, respectively (Petrov *et al.* 2005).

Due to flooding, snowmelt or liquid precipitation, slush forms in the snow pack and may further freeze into snow-ice. Because of the low heat conductivity of the snow on top, the slush does not freeze through quickly and a slush layer may be captured in the ice interior for longer periods (e.g. Leppäranta 2009). These slush layers serve as habitats for biota. Snow-ice layers are common in Lake Vendyurskoe, and the average thicknesses of snow-ice and congelation ice reach 21–27 cm and 35–50 cm, respectively. In severe winters with little snow (as in 1999), the congelation ice thickness is more than 50 cm while snow-ice thickness is less than 10 cm (Petrov *et al.* 2005).

Data collected

The field campaigns were performed in April 2006 and April 2007. The data include the solar radiation transfer through the snow and ice, weather, snow and ice thickness and vertical profiles of water temperature (Table 1). There was an actinometric station and two measurement lines along the lake axes for spatial variations (Figure 1). The station data include global radiation and Photosynthetically Active Radiation (PAR), which covers the 400–700 nm band. The so-called visible light band is 380–760 nm, close to the PAR band. The campaigns included three surveys (April 18, 24 and 27) in 2006 and two surveys (April 16 and 19) in 2007 along the measurement lines.

At the actinometric station, the downwelling and upwelling planar irradiances at the surface (E_d and E_u, respectively) were measured with a Star-shaped pyranometer (Theodor Friderich & Co, Meteorologische Gerate und Systeme, Germany). Planar irradiance refers to the radiance falling on a plane; downwelling planar irradiance comes from the upper hemisphere and upwelling irradiance comes from the lower hemisphere (Dera 1992). The downwelling planar irradiance beneath the ice was measured

Table 1 | Data collected in Lake Vendyurskoe during 2006 and 2007 campaigns

Quantity	Device/sensor	Range	Accuracy
Global radiation, $W\,m^{-2}$			
-surface	Star-shaped	0–1000	1 ± 10%
-under ice	pyr. M-80 m	0–1000	0.3 ± 20%
PAR, $\mu mol\,m^{-2}\,s^{-1}$	MDS-L	0–5000	10 ± 0.4%
Air temperature, °C	EMS32A	−20 to +60	±0.3
Air humidity, %	EMS32A	0–100	±2.5
Wind speed, $m\,s^{-1}$	MetOne 034	0–20	±0.1
Wind direction, deg	MetOne 034	0–360	±4
Cloudiness	Visual	0–1	1/8
Water temperature, °C	CTD-90M	−2 to +32	±0.005

with a device using M-80 m universal pyranometer produced in Russia. These instruments were inter-calibrated, and the ratio of Star irradiance to M-80 m irradiance was found to be equal to 1.0003. The albedo was measured with the M-80 m universal pyranometer and a digital millivoltmeter along the 4-cross-section (Figure 1). The meteorological parameters were registered with the weather station (EMS, Czech Republic) and water temperature soundings were made with the CTD-90M profiler (ASD Sensortechnik GmbH, Germany). In addition, cloudiness was visually estimated in 2007. The equipment capacities are shown in Table 1. The depths of snow and ice were measured with a metre stick and the distinction of snow-ice from congelation ice was determined from ice samples.

The transfer of PAR through the ice cover was recorded by installing small sensors (MDS-L, Alec Electronics Co. Ltd., Japan) into the ice. The sensors have been calibrated by the manufacturer for the downwelling scalar quantum irradiance q_{d0} in the PAR band. Scalar quantum PAR irradiances are used in biological investigations since they provide the number of photons available for primary production. For isotropic radiation conditions, the ratio of downwelling (or upwelling) scalar irradiance to planar irradiance is 2.

Figure 2 shows the PAR sensor response curve; the calibration constants to evaluate PAR differ for measurements in air and water. This quantity gives the flux of light quanta and its unit is quanta $m^{-2}\,s^{-1}$, normally given in $\mu mol\,m^{-2}\,s^{-1}$ ($1\,\mu mol = 6.022{\cdot}10^{17}$ quanta), defined as (e.g. Arst 2003):

$$q_{d0}(z) = \int_{PAR} \frac{\lambda}{hc} E_{d0}(z;\lambda)\,d\lambda \quad (1)$$

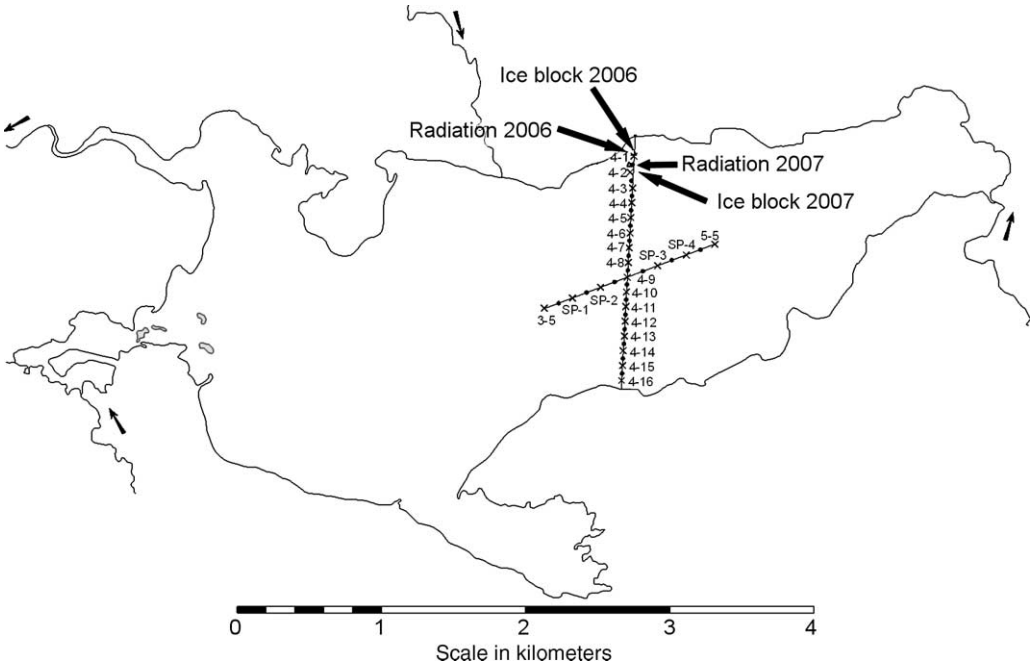

Figure 1 | The locations of measurement stations during field campaigns in 2006–2007.

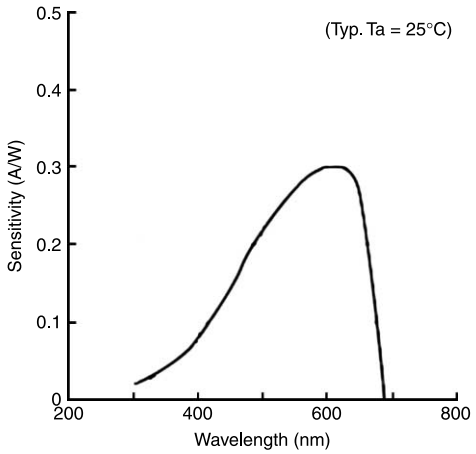

Figure 2 | The spectral sensitivity (A/W) of the PAR sensors as a function of wavelength. A is the electric current detected by the photodiode in Amperes and W is the incident radiation in Watts.

where z is depth, λ is wavelength, h is Planck's constant, c is the velocity of light in vacuum and E_{d0} is downwelling scalar irradiance power. To transform between broadband irradiance power and quantum irradiance, in the atmosphere $q_{d0}/E_{d0,PAR} = 4.60\,\mu mol\,J^{-1}$ where $E_{d0,PAR}$ is the scalar PAR irradiance power. In Finnish and Estonian lakes, the ratio increases to $4.8–5.5\,\mu mol\,J^{-1}$ with large values for more turbid lakes (Reinart *et al.* 1998); $5.0\,\mu mol\,J^{-1}$ can be taken as a representative value in the present study.

The physical size of the PAR sensor is 115 mm in length and 18 mm in diameter, with the sensor unit on top. The installation was done by cutting and lifting up an ice block with approximately 0.5×0.5 m horizontal cross-section, drilling holes from the bottom of the block for the sensors and finally putting the block back with the sensors. The sensors were fastened in the holes with slush filling, and the deepest sensors were initially located at their length (12 cm) from bottom. They recorded the irradiance at 10-minute intervals. Due to melting and freezing, the sensor positions changed relative to the ice top and bottom boundaries. The 2007 PAR data turned out to have calibration problems and they were consequently excluded from the analysis.

The weather conditions were typical for April during the field campaigns. The air temperature was positive in the daytime and negative in the night, accompanied by high humidity. Wind velocity was mostly low, not more than $4\,m\,s^{-1}$. Cloudiness in April 2007 (not measured in 2006) was sometimes rather high, up to 8/8 (100%) resulting in low incoming solar radiation levels, down to $200\,W\,m^{-2}$ at noon on April 18. In April 2006, the snow cover was already quite thin (not more than 3 cm) during the first survey. Six days later (April 24), it had melted nearly everywhere except for a few spots close to the northern shore, leaving a solid snow-ice surface. On April 27, the final melting stage started with liquid water (dark) spots scattered on the surface. During the first survey (April 16 2007), the surface of the snow-ice was covered by a layer of snow pellets about 3 mm thick on average. Close to the northern shore, the height of such snow spots was about 1 cm. In three days, the surface was covered by water-saturated snow pellets.

RESULTS

Ice and snow thickness

Ice and snow thickness surveys were performed along the measurement lines (Figure 1) for their spatial variations (Table 2; Figure 3). In 2006 the thickness of ice decreased by 12.8 cm in nine days: 10.8 cm was snow-ice melting at the top surface and 2.0 cm was bottom melting. These values correspond to mean melt rates of 1.2 cm day^{-1} at the ice surface and 0.2 cm day^{-1} at the bottom of the ice. In the following year the ice thickness decreased by 6.2 cm in three days, corresponding to the mean melt rates of 1.2 cm day^{-1} again for the snow-ice and 0.8 cm day^{-1} for congelation ice.

Melting of ice by Δh requires heat of $\rho L \Delta h$, where ρ is ice density and L is the latent heat of freezing. For a melt rate of 1.0 cm day^{-1}, the heat flux must be $35\,W\,m^{-2}$. This means that during the daylight hours, the net solar energy flux must be around $100\,W\,m^{-2}$ and the heat flux from the water at least $7\,W\,m^{-2}$. This lower limit was obtained in 2006 and agrees with Bengtsson *et al.* (1996). The large value in 2007 ($29\,W\,m^{-2}$) may be due to better transparency of the thin ice and returning solar heat flux from the water to the ice bottom. The thickness changes do not provide an indication of internal melting, which is indirectly obtained from solar radiation measurements.

Table 2 | Average and standard deviation (in parenthesis) of ice and snow thickness (cm) and albedo in Lake Vendyurskoe in the study periods. The statistics are based on the measurement lines across the lake in 24 sites (Figure 1)

Date	Total ice	Congelation ice	Snow-ice	Snow	Albedo
18 April 2006	51.5 (3.6)	31.2 (5.7)	20.3 (3.2)	1.7 (1.2)	n/a
24 April 2006	44.5 (3.7)	29.7 (5.7)	14.8 (3.3)	0*	0.41 (0.05)
27 April 2006	38.7 (3.6)	29.2 (5.7)	9.5 (2.8)	0 (0)	0.27 (0.03)
16 April 2007	38.1 (1.6)	31.2 (2.3)	6.9 (1.5)	0.4 (0.4)	0.20 (0.04)
19 April 2007	31.9 (2.0)	28.7 (2.3)	3.2 (1.7)	0 (0)	0.35 (0.02)

*Thin snow in 3 sites out of the 24.

The variability was largest for congelation ice thickness (Table 2). The variance of total ice thickness is less than the variance sum of the thicknesses of the congelation and snow-ice layers as these layer thicknesses are correlated (the correlation coefficient was -0.22). The variability of a given layer was almost constant in both years; i.e. the progress of melting did not increase or decrease the variability of the layer thicknesses. This last conclusion is not likely to hold to the end of the melting season. In snow-ice formation by flooding, roughly half of the mass comes from snow (Leppäranta & Kosloff 2000). A 20 cm snow-ice layer therefore contains about 100 mm water equivalent of snow, corresponding to 30–40 cm snow accumulation.

Solar radiation balance at the surface

The difference and ratio of downwelling and upwelling global irradiances at the surface,

$$E_n = E_d - E_u \tag{2a}$$

$$\alpha = \frac{E_u}{E_d}, \tag{2b}$$

give the net solar radiation absorbed by the lake and the albedo. In 2006 the peak level at noon was usually 300–500 $W\,m^{-2}$, with one day as high as 600 $W\,m^{-2}$ and for two days as low as 100 $W\,m^{-2}$ (Figure 4). The minima are from cloudy days, and otherwise the peaks show a slow increase. In 2007 the level of net radiation was lower and the increase much stronger than in the previous year.

The main factors influencing the downwelling and upwelling irradiances are the albedo and the directional distribution of the incoming radiation, which depends on solar altitude and cloudiness. The role of the albedo is best seen when comparing cases with similar solar altitude and cloudiness. In the present cases, both albedo and cloudiness caused major variations in the net radiation. According to a common formula to estimate the incoming solar radiation

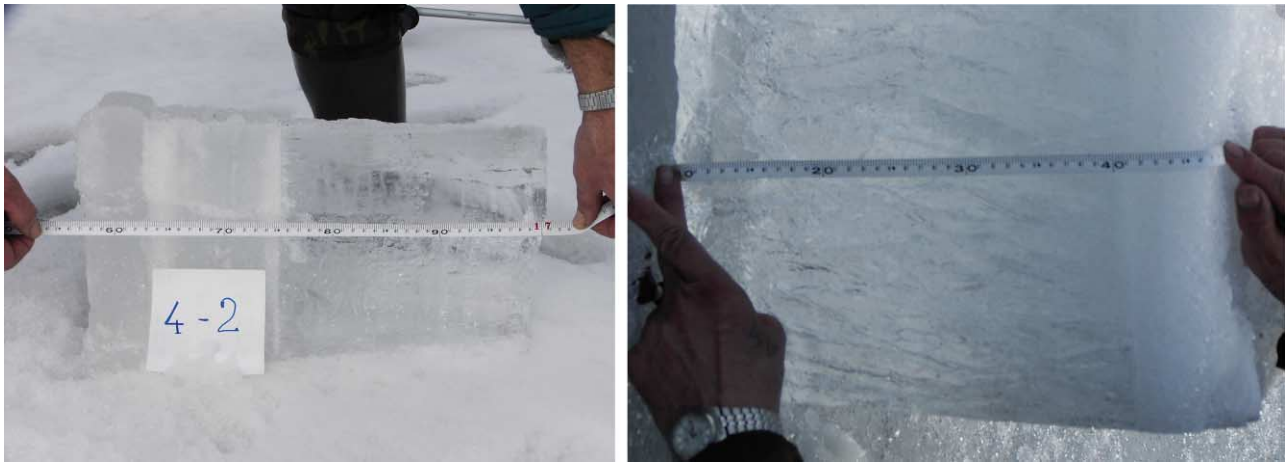

Figure 3 | Ice samples from 2006 (left, with top surface on left) and 2007 (right, with top surface on right). In the left photograph, the notation 4-2 refers to the site shown in Figure 1.

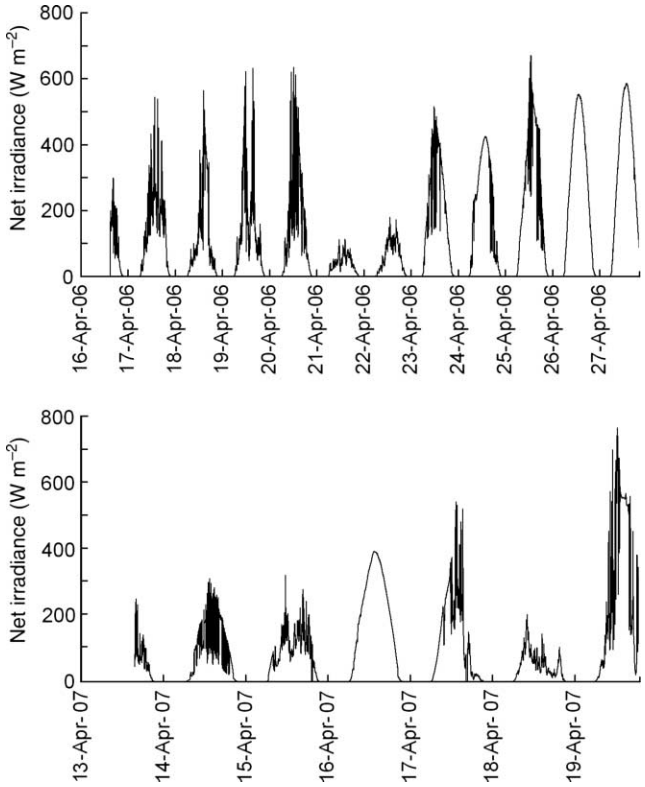

Figure 4 | Net irradiance at the surface in 2006 and 2007.

on the basis of location and time (Zillman 1972) and cloudiness (Reed 1977), on April 20 the noon peak should be 700 W m^{-2} under clear skies and 300 W m^{-2} under overcast conditions. The limits were satisfied by the present data except for one very narrow peak at 800 W m^{-2} and one overcast day with incoming radiation down to 200 W m^{-2}.

At the beginning of the study periods there was only a thin layer of snow. The albedo was therefore already small: below 0.5 (Figure 5; Table 2). In both years the albedo decreased steadily due to the increasing wetness of the surface; at the end it was down to 0.1. Daily variability was also seen due to solar altitude and cloudiness variations. The values obtained are lower than usually assumed in thermodynamic ice models. The daily variability of albedo was quite large due to the evolution of the surface state during the daytime, changing solar altitude and cloudiness conditions. The spatial standard deviation of the albedo was 10% of its absolute value. The influence of solar altitude on the albedo should show albedo minimum at solar noon and albedo maximums at sunrise and sunset; this is seen on some days but normally masked by other factors. In Lake Venduyurskoe, measurements have shown that solar radiation under ice may differ by 30% at two stations spaced 1.2 km apart. Layers of snow and ice of depths 15–20 cm and 40 cm reduce about 90 and 80%, respectively, due to solar radiation coming onto the upper boundaries (Petrov *et al.* 2005).

One PAR sensor was deployed at the surface to measure the PAR band downwelling scalar quantum irradiance. For the comparison with downwelling planar irradiance, there are three correction factors (e.g. Arst 2003): (1) ratio of quantum irradiance to irradiance power is $q_{d0}/E_{d0,PAR} = 4.6\,\mu mol\,J^{-1}$, assuming white light spectrum; (2) ratio of scalar irradiance to planar irradiance is $E_{d0}/E_d \approx 2$, obtained by integrating the radiances with common directional distribution (exactly 2 for diffuse radiation); and (3) ratio of PAR irradiance to global irradiance is $E_{d,PAR}/E_d \approx 0.44$ (Bird & Riordan 1986). The numerical value of the PAR sensor recording should therefore be about four times the numerical value of the global radiation sensor, i.e. $q_{d0}/E_d \approx 4\,\mu mol\,J^{-1}$. In 2006 the result was rather

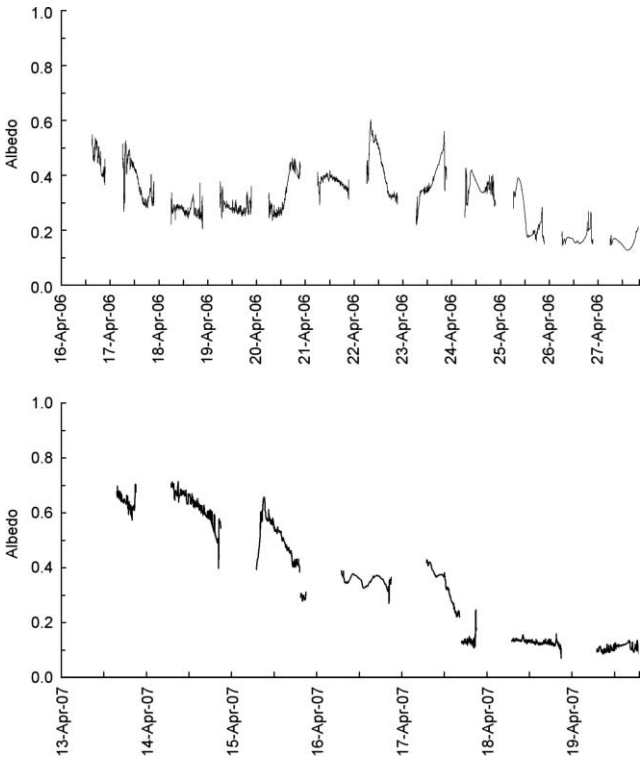

Figure 5 | Time series of the albedo in 2006 and 2007.

consistent with these correction factors; the daily ratios q_0/E_d averaged to 4.8 μmol J^{-1} and the standard deviation was 0.3 μmol J^{-1}. In 2007, however, the average and standard deviation were 7.2 μmol J^{-1} and 1.0 μmol J^{-1}, for reasons so far unknown to us. Due to this problem the 2007 PAR data was not used further in this work.

Transfer of sunlight through ice and snow

The vertical z-axis is taken as positive down. The downwelling solar irradiance $E_d(z)$ attenuates when going down into the snow and ice and water, given by:

$$\frac{dE_d}{dz} = -\kappa E_d \tag{3}$$

where $\kappa = \kappa(z)$ is the diffuse attenuation coefficient. The solution is:

$$E_d(z) = (1-\alpha)E_d(0)\exp\left(-\int_0^z \kappa dz'\right). \tag{4}$$

Because of the high albedo of snow and ice, the level of net irradiance is drastically reduced by the ice cover compared to the open water season. Only visible light and narrow sections of ultraviolet and infrared radiation penetrate into water ice or snow for more than a few centimetres. According to these characteristics, the net solar radiation is divided into surface absorption and penetrating parts. Shorter and longer wavelengths are absorbed fast and virtually only the PAR band is left beneath the ice.

The light transmissivity of the ice cover is defined here as:

$$\tau = \frac{E_d(H^+)}{E_d(0^+)} = \frac{E_d(H^+)}{(1-\alpha)E_d(0^-)} \tag{5}$$

where $H = h_i + h_s$ is the total thickness of ice (h_i) and snow (h_s) and the upper indexes + and – refer to the right and left sides, respectively, with respect to the z-coordinate direction. Since this direction is down, the index + refers to below and the index–to above the indicated depth.

The reason for the definition given by Equation (5) rather than the more common one, $\tau_0 = (1-\alpha)\tau$, is that we can focus on the internal properties of the ice itself. In 2006 the level was stable and normal in the range $\tau \approx 0.2$–0.3 with extremes at 0.1 and 0.4 (Figure 6). The low levels were obtained in early morning hours while the peaks were reached in afternoons, which can be partly explained by the influence of solar altitude. The improvement of transmissivity due to a decrease in ice thickness was compensated in the evolution of the internal structure of the ice so that no trend resulted. In 2007, the development was quite different. The transmissivity increased steadily during the six days from 0.1 to 0.5. The ice was 10–15 cm thinner in 2007; a greater transmissivity by about 0.1 compared to 2006 would result if the ice sheets were optically similar. This optical similarity was true to some degree, but there was a large difference in the time evolution.

A lake ice sheet is optically stratified, and a three-layer approach–snow, snow-ice and congelation ice–gives the transmissivity as:

$$\tau = \exp[-(\kappa_s h_s + \kappa_{si} h_{si} + \kappa_i h_i)] \tag{6}$$

where κ and h are the thickness and attenuation coefficient with the subscript s, si or i for snow, snow-ice or congelation ice, respectively. If the bulk transmissivity is known from measurements above and beneath the ice, the attenuation coefficients of the sub-layers can be obtained by linear regression techniques from Equation (6). Taking logarithms of both sides results in a linear form for the unknowns, κ_i, κ_{si}, and κ_s. A necessary and sufficient condition for their estimation is that the layer thicknesses form a linearly independent set and the number of cases is at least three. Since the snow layer was almost absent in both years, only the snow-ice and congelation ice layers can be considered in the present case. The result of parameter estimation using the data of both years is: $\kappa_i = 0.017$ cm^{-1} and $\kappa_{si} = 0.06$ cm^{-1} corresponding to the attenuation (e-folding) depths of 60 cm and 15 cm.

The PAR sensors produced time series at several depths for a more detailed picture of the radiation transfer in 2006 (Figure 7). The initial sensor depths were zero, 14 cm and 39 cm, and the ice sensors were at the interface of snow-ice and congelation ice and 25 cm into the congelation ice. In the first half, the attenuation of the signal corresponds well with what was obtained with the pyranometers; in the

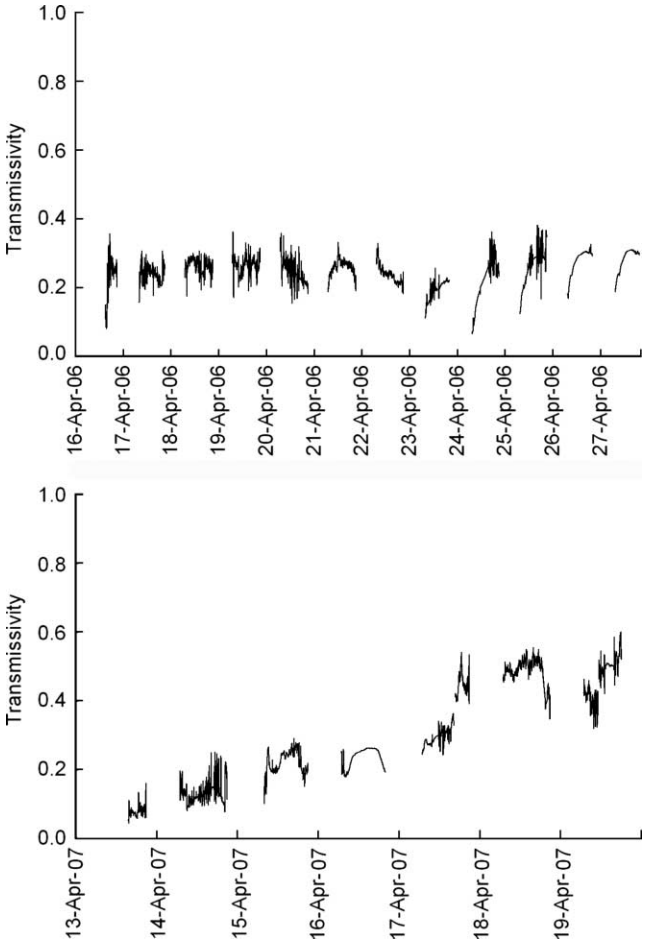

Figure 6 | The transmissivity of ice in the experiments 2006 (April 16–27) and 2007 (April 13–19) based on the pyranometer data.

second half the data is more uncertain due to the melting and deterioration of the ice. The attenuation depths were estimated as 80 cm for congelation ice and 15 cm for snow-ice. Compared with the method based on transmissivity data, the difference in congelation ice may be due to measurement method (planar and scalar irradiance) or measurement band (PAR and global radiation).

The diffusiveness of the light in the ice was mapped by comparing the ratio of upwelling and downwelling irradiances using two PAR sensors, initially deployed into a depth of 29 cm. The result (Figure 8) gave the average ratio as $q_{u0}/q_{d0} = 0.58$. The different spectral distributions of upwelling and downwelling irradiance, together with the calibration curve (Figure 2), may have slightly influenced the result.

Light attenuation in clear congelation ice is of the same magnitude as in the liquid lake water, $\kappa \sim 1\,\mathrm{m}^{-1}$. This is a

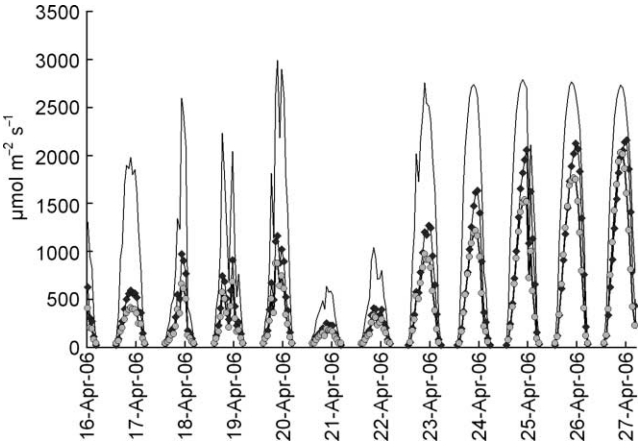

Figure 7 | Quantum downwelling PAR irradiance (μmol m^{-2} s^{-1}) in the surface, snow-ice and congelation ice in April 16–27, 2006; the depths were 0, 14 and 39 cm in the beginning, 0, 3, and 28 cm at the end (due to surface melt).

non-trivial fact, confirmed by observations, as the nature of the absorption and scattering/backscattering processes is different in water to that in congelation ice. However, in highly humic lakes, short wavelengths are absorbed more strongly in liquid water. Lake Vendyurskoe has a Secchi depth of 3–4 m, which corresponds to the attenuation (e-folding) depth of 1.2–1.6 m (Arst *et al.* 2008), twice as much as obtained here for the congelation ice (0.6 m). Gas bubbles in the ice scatter light that lowers the transparency and flattens the attenuation spectrum but, on the other hand, congelation ice contains smaller quantities of other optically active substances (e.g. coloured dissolved organic matter or CDOM, chlorophyll *a* and suspended matter); this means better transparency. Impurities are mostly rejected in congelation ice growth, while lake water is trapped into the freezing slush in snow-ice formation by flooding.

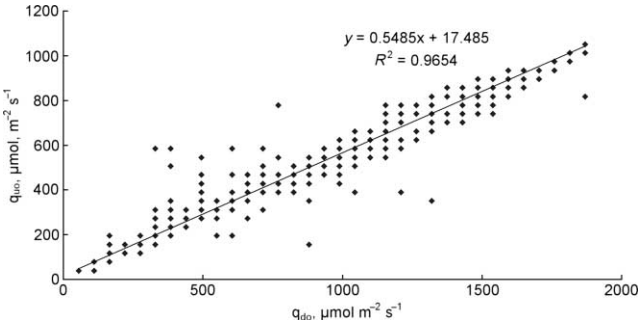

Figure 8 | Upwelling versus downwelling irradiance in the ice sheet for quantum scalar PAR irradiance; the sensor depth was 29 cm in the beginning, 18 cm at the end.

However, ice crystal structure and gas bubbles dominate the light transfer and the CDOM, chlorophyll or suspended matter signals do not become identifiable in the light attenuation spectrum (Arst *et al.* 2008).

Light conditions beneath a lake ice cover are usually reduced compared to the open water season. In the case of bare congelation ice, the light level is lowered due to the surface albedo. Snow on the ice makes a big difference; e.g. adding 15 cm snow to a 50 cm ice sheet lowers the irradiance level beneath the ice by one order of magnitude. The euphotic depth (z_e) is normally taken as the depth where the irradiance level has reduced to 1% of that at the surface (Arst 2003). In open water conditions, this is given by $z_e = \ln(100)/\kappa$. In the presence of snow and ice, this definition contains a major problem as it does not include the albedo. To correspond to a similar photon flux in ice and open water seasons, a preferable definition of the euphotic depth is $z_e = \ln[100(1-\alpha)\tau]/\kappa$. If there is more than 20 cm of snow on the ice, no photosynthesis is possible in the upper layers of the water column.

When ice melting progresses, the light transmissivity tends to increase due to thinning of the ice sheet. In particular, melting at the top layer takes out snow-ice which has lower transmissivity. Changes in the structure of congelation ice may increase or decrease the transmittance as more porous ice is less transparent, in particular when the pores contain gas bubbles. However, the present data does not reach the phase when the transparency increased from ice structure evolution and therefore this question remains open.

Heat budget in the melting season

The surface heat balance is written:

$$Q_n = (1-a)(1-\gamma)Q_s + Q_{nL} + Q_T + Q_P \quad (7)$$

where Q_n is the net heating, γ is the fraction of solar radiation penetrating the surface, Q_{nL} is net terrestrial radiation, Q_T is the turbulent heat flux and Q_P is the heat from precipitation. Heat available for internal melting is $Q_i = (1-\alpha)\gamma(1-\tau)Q_s$.

Figure 9 presents the surface radiation budget. The turbulent fluxes were small and there were no significant

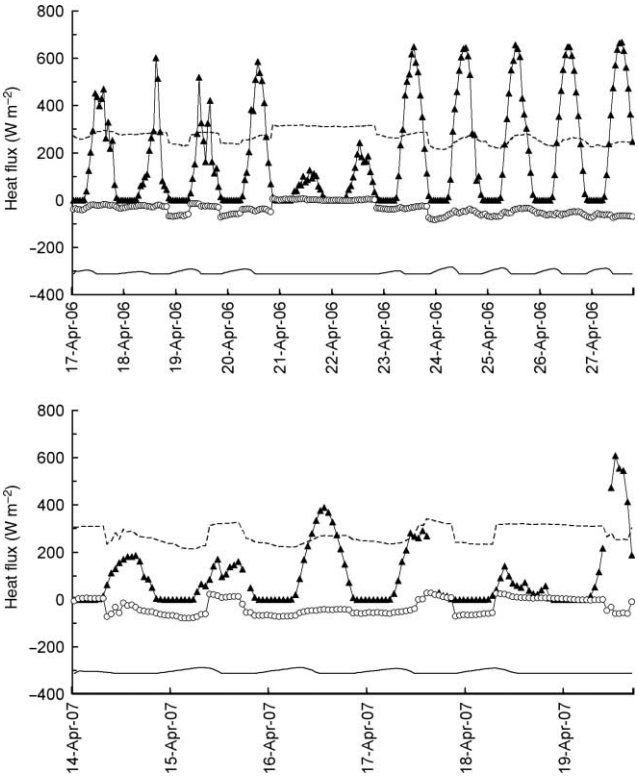

Figure 9 | Surface radiation budget in 2006 and 2007 experiments: net solar radiation (▲—▲), thermal radiation emitted by the surface (———), thermal radiation from the atmosphere (- - - - -), and net terrestrial radiation (= = = = =).

precipitation events in both years. In April 2006, the terrestrial radiation loss at night was 50–100 W m^{-2} while in the daytime the solar radiation was dominant. In April 2007, the situation appeared to be different. During three days (14, 15 and 18 April), the net terrestrial radiation exceeded solar radiation even in daytime. In fact, there are many uncertainties in evaluating the radiation from atmospheric data in the present cases. The use of surface melting is therefore the best representation of the net flux at the surface.

The daily ice heat budgets are presented in Table 3. Ice thickness observations (Table 2) show that surface melting was stronger than bottom melting. The mean surface melt rate was 1.2 cm day^{-1} in 2006 and in 2007, while the mean bottom melt rates were 0.2 cm day^{-1} and 0.8 cm day^{-1} in these years. The net solar radiation penetrating into the ice was 100–200 W m^{-2} in clear or half-clear days. With a transparency of 0.25–0.5, the daily energy absorbed by

Table 3 | Heat budget of the ice in 2006 and 2007 experiments. The daily mean heat fluxes are presented ($W m^{-2}$), and also shown is the daily mean temperature (°C). Note that melting 1 cm of ice needs mean flux of $35.4 W m^{-2}$

	Net surface heat flux	Internal heating	Bottom heat flux	Net flux	Air temperature
2006					
April 18	32	40	9	81	2.5
April 19	32	45	9	86	3.5
April 20	32	60	9	101	4
April 21	32	15	9	56	2.5
April 22	25	20	9	54	2
April 23	25	75	8	108	2.5
April 24	44	75	7	126	2
April 25	44	90	6	140	5
April 26	62	105	6	173	4.5
2007					
April 16	44	70	29	143	2.5
April 17	44	40	29	113	4
April 18	44	15	29	88	5

the ice sheet was $50–150 W m^{-2}$, significantly more than the surface and bottom melting together ($40–70 W m^{-2}$).

When the ice is optically thick, half of the net solar radiation is used for the internal melting and half for the surface melting. When the optical thickness decreases, an increasing portion of the net radiation penetrates the ice and warms the water under the ice, resulting with increased bottom heat flux. In 2006, the bottom heat flux increase was not very significant since the total stayed at $7.8 W m^{-2}$; in 2007, however, the increase was $20 W m^{-2}$.

The melting of ice can be described in terms of ice volume (V) change as:

$$\frac{dV}{dt} = \frac{d(\nu h)}{dt} = \nu\left(\frac{dh_{surface}}{dt} + \frac{dh_{bottom}}{dt}\right) + h\frac{d\nu}{dt} \quad (8)$$

where ν is ice porosity. Thickness observations give the first term on the right-hand side and the second term can be estimated from solar radiation data, simply as:

$$\frac{d\nu}{dt} = \frac{Q_i}{\rho h L} = \frac{(1-\alpha)Q_s}{\rho h L}[1 - \exp(-\kappa h)]. \quad (9)$$

Internal melting is a very important factor in the ice break-up. It is about the same as or more than the surface melting. For physical understanding of the melting process, internal melting therefore needs to be tracked. Net solar radiation provides an indication of the volume of ice melt, but does not differentiate how the melt is distributed in the ice sheet. Internal melting changes the optical properties of ice and the strength of the ice, thus influencing the thermal and mechanical ice break-up.

Sea ice measurements have shown that the flexural strength has decreased by one order of magnitude at porosity of 0.15 (Weeks 1998). We may anticipate that when the porosity of melting lake ice approaches the coarse packing density of balls, $\pi/6 \approx 0.5$, the ice cannot bear its own weight but breaks into the water body. For example, for 50 cm ice, internal melting corresponding to 2 cm day^{-1} reaches critical porosity in 10 days. In this period, the ice thickness has reduced by 10 cm if the surface and bottom melting sum to 2 cm day^{-1}. The ratio of internal melting to boundary melting depends on the relative strength of solar radiation in the heat balance. Here the ratio was about the same for the two melting seasons.

Also shown in Table 3 is the daily mean air temperature T_a, which is a common index in ice melting calculations. The so-called degree-day method gives the melt rate as $\dot{h} = AT_a$, where A is the degree-day coefficient. The present data give $A = 0.32$ cm $day^{-1}{}^{\circ}C^{-1}$; however, the correlation

coefficient is only 0.41. This is small due to the fact that air temperature is an indirect indicator of melting only.

Sunlight also plays a major role in the water body. At ice break-up, the bulk water temperature can be as high as 4°C leaving just a thin layer of cold water beneath the ice. Under these conditions, the spring overturn may be very short or even absent in some extreme years. Two scenarios can be expected in the development of the water temperature after the ice break-up, illustrated by earlier data from this lake. In the first case (Figure 10(a)), the temperature of the whole water column drops down below 4°C (the bottom layers are warmer by then), the water temperature becomes quasi-homogeneous and the water warms due to solar heating. The classical spring overturn takes place providing a full mixing of the water column; the duration of this process is 3–5 days. The drastic heat loss is likely produced by ice melting. In the second case (Figure 10(b)), the water temperature reaches 4°C almost within the whole water column, except in the bottom layers where its value is already well above. The water then warms until the whole water column has become quasi-homogeneous. The temperature difference is compensated for the density by the higher salt content in bottom waters (Malm *et al.* 1997) providing stability of the bottom layers. The overturn therefore does not take place, and the fingerprints of 'winter' processes may remain in bottom layers until the first full mixing, if any.

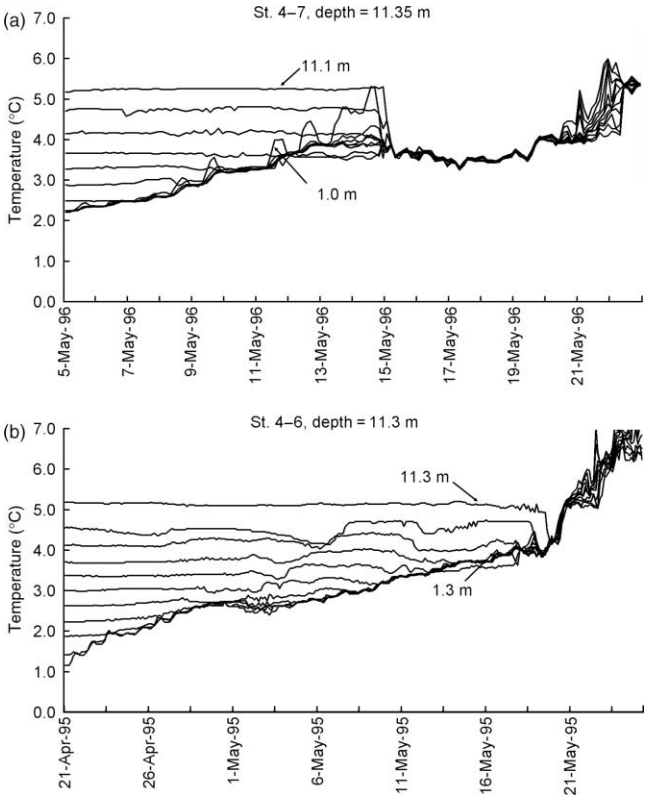

Figure 10 | The vertical temperature development in Lake Vendyurskoe: (a) May 5–25, 1996 and (b) April 21–May 31, 1995 from observational data (thermistor chains). The top lines correspond to the depth in the vicinity of bottom.

DISCUSSION

The number of publications regarding the physics of lake ice is not very large. This is particularly so for the melting season, which is where this research focuses on. What exists is more related to simple ice growth models and climatology.

Wright (1964) reported an attenuation coefficient of $2.5-3\,m^{-1}$ for irradiance in lake ice and about 15 cm for snow. For several lakes in Estonia and Finland, Leppäranta *et al.* (2003) and Arst *et al.* (2006) reported a range of $0.5-2\,m^{-1}$ for most lakes but ice structure information was limited. They also concluded that ice may be more or less transparent than water of the same lake, and that the transmissivity depends strongly on the ice stratification and gas bubbles, which vary from one season to another. There are therefore no lake-specific ice transmissivities. For ice in the Arctic seas, the attenuation coefficient for congelation ice is $\sim 1\,m^{-1}$ and for 'white ice' is $5-10\,m^{-1}$ (Perovich 1998). Investigations of the melting rate for lake ice are based on the heat budget or degree-days, but do not break down into surface, bottom and internal components (Ashton 1986). In a very recent study in Lake Pääjärvi, Finland, similar characteristics for the melting season were obtained (Jakkila *et al.* 2009).

A theoretical model for optical properties of lake ice was presented by Mullen & Warren (1988). The optically active impurity was gas bubbles and the main focus was in the albedo of lake ice. A major issue was the shortage of good field data. This work, with a very few similar recent studies, has approached the problem from field investigations which will be important in the fine-tuning of lake optics models in future.

CONCLUSIONS

Field experiments were performed during the ice melting period. The purpose was to examine the evolution of albedo and light transfer through ice and snow, ice melt rate and light conditions beneath the ice cover. In 2006, the total ice thickness decreased by 12.8 cm in 9 days and by 6.2 cm in 3 days in the following year.

The following conclusions are drawn.

1. The mean melt rate was 1.2 cm day^{-1} at the surface, 0.2–0.8 cm day^{-1} at the bottom and 1–2 cm day^{-1} thickness equivalent in the interior. The large bottom melt rates are probably due to better transparency of thin ice and returning of the solar heat flux from water to the ice bottom.
2. The heat budget was governed by solar radiation, net daily peaks up to 400–500 W m^{-2} in clear days.
3. Albedo decreased from 0.5–0.8 for wintertime dry ice/snow surface to 0.1 for spring wet bare ice surface. The spatial standard deviation of the albedo was about 10%.
4. A method was presented to obtain attenuation coefficients for ice cover layers from radiation measurements above and below the ice. The data need to contain linearly independent layer thickness combinations.
5. The e-folding depth of light level was 60–80 cm for congelation ice and 15 cm for snow-ice. The transmissivity of ice cover varied within 0.25–0.35 in 2006 (ice deterioration decreased attenuation depth and melting decreased attenuation distance) while in 2007 there was a systematic trend from 0.1 to 0.5 in 6 days.

Lake ice melting period has not been largely investigated, mostly because of safety issues and logistical problems. Our results therefore contain a significant addition to lake ice knowledge. Here, the evolution of albedo and transmissivity were quantified for the melting period when they were undergoing drastic changes. The radiation budget is a major issue for ice melting, for warming the water beneath ice and for the start-up of biological production in spring. The data allowed us to decompose the melt rate into surface, bottom and internal portions. This is critically important information for mathematical modelling of lake ice melting and for evaluating ice strength, predicting the breakage of the ice cover and evaluating its consequences.

ACKNOWLEDGEMENTS

The authors would like to express their gratitude to Andrei Mitrokhov, Nikolai Palshin, Maksim Potakhin and Roman Zdorovennov for the efforts in collecting observational data, to Galina Zdorovennova for help with the figures and to Mary-Juen Sohn for checking the English language. Financial support was provided to Matti Leppäranta from Vilho, Yrjö and Kalle Väisälä Foundation of the Finnish Academy of Sciences and the Academy of Finland and to Arkady Terzhevik from the Russian Foundation of Basic Research (Project 07-05-00351), Russian Academy of Sciences and NATO Programme *Security Through Science* (project ESP.NR.NRCLG 982964).

REFERENCES

Arst, H. 2003 *Optical Properties and Remote Sensing of Multicomponental Water Bodies*. Springer–Praxis, Chichester, UK.

Arst, H., Erm, A., Leppäranta, M. & Reinart, A. 2006 Radiative characteristics of ice-covered fresh- and brackish-water bodies. *Proc. Estonian Acad. Sci. Geol.* **55**, 3–23.

Arst, H., Erm, A., Herlevi, A., Kutser, T., Leppäranta, M., Reinart, A. & Virta, J. 2008 Optical properties of boreal lake waters in Finland and Estonia. *Boreal Environ. Res.* **13**(2), 133–158.

Ashton, G. (ed.). 1986 *River and Lake Ice Engineering*. Water Resources Publications, Littleton, Co.

Bengtsson, L., Malm, J., Terzhevik, A., Petrov, M., Boyarinov, P., Glinsky, A. & Palshin, N. 1996 Field investigations of winter thermo- and hydrodynamics in a small Karelian lake. *Limnol. Oceanogr.* **41**, 1502–1513.

Bird, R. E. & Riordan, C. J. 1986 Simple solar spectral model for direct and diffuse irradiance on horizontal and tilted planes at the Earth's surface for cloudless atmospheres. *J. Clim. Appl. Meteorol.* **25**(1), 87–97.

Dera, J. 1992 *Marine Physics*. Elsevier, Amsterdam.

Jakkila, J., Leppäranta, M., Kawamura, T., Shirasawa, K. & Salonen, K. 2009 Radiation transfer and heat budget during the ice season in Lake Pääjärvi, Finland. *Aquatic Ecology*, **43**, 681–692..

Leppäranta, M. 2009 Modelling the formation and decay of lake ice. In George, G. (ed.), *Climate impact on European lakes*. Aquatic Ecology Series, Vol. 4. Springer-Verlag, Germany.

Leppäranta, M. & Kosloff, P. 2000 The thickness and structure of Lake Pääjärvi ice. *Geophysica* **36**(1–2), 233–248.

Leppäranta, M., Reinart, A., Arst, H., Erm, A., Sipelgas, L. & Hussainov, M. 2003 Investigation of ice and water properties and under-ice light fields in fresh and brackish water bodies. *Nord. Hydrol.* **34**, 245–266.

Litinskaya, K. D. & Polyakov, Yu. K. 1975 Lakes of Vendyurskaya group – Uros, Rindozero, Vendyurskoe. In *Water resources of Karelia and their use*, Petrozavodsk, pp. 57–66 (in Russian).

Malm, J., Terzhevik, A., Bengtsson, L., Boyarinov, P., Glinsky, A., Palshin, N. & Petrov, M. 1997 Temperature and salt content regimes in three shallow ice-covered lakes: 1. Temperature, salt content, and density structure. *Nord. Hydrol.* **28**, 99–128.

Mullen, P. C. & Warren, S. G. 1988 Theory of optical properties of lake ice. *J. Geophys. Res.* **93**(D7), 8303–8414.

Perovich, D. K. 1998 The optical properties of the sea ice. In: Leppäranta, M. (ed.), *Physics of Ice-Covered Seas*. Helsinki University Printing House, Helsinki, pp. 195–230.

Petrov, M., Terzhevik, A., Palshin, N., Zdorovennov, R. & Zdorovennova, G. 2005 Absorption of Solar Radiation by Snow-and-Ice Cover of Lakes. *Vodnye Resursy*, **5**, 496–504. (in Russian, English transl. in *Water Resources*).

Reed, R. 1977 On estimating insolation over the ocean. *J. Phys. Oceanogr.* **7**, 482–485.

Reinart, A., Arst, H., Blanco-Sequeiros, A. & Herlevi, A. 1998 Relation between underwater irradiance and quantum irradiance in dependence on water transparency at different depths in the water bodies. *J. Geophys. Res.* **103**(C4), 7749–7752.

Wang, C., Shirasawa, K., Leppäranta, M., Ishikawa, M., Huttunen, O. & Takatsuka, T. 2005 Solar radiation and ice heat budget during winter 2002–2003 in Lake Pääjärvi, Finland. *Verh. Internat. Verein Limnol.* **29**, 414–417.

Weeks, W. F. 1998 Growth conditions and structure and properties of sea ice. In: Leppäranta, M. (ed.), *The Physics of Ice-covered Seas*, (Vol. 1). Helsinki University Press, Helsinki, pp. 25–104.

Wright, R. T. 1964 Dynamics of phytoplankton community in an ice-covered lake. *Limnol. Oceanogr.* **9**, 163–178.

Zillman, J. W. 1972 *Study of some aspects of the radiation and heat budgets of the southern hemisphere oceans*. Bureau Meteorol., Dept. Inter., Meteorol. Stud. Rep. 26.

First received 1 December 2008; accepted in revised form 11 August 2009. Available online December 2009.